

# A Hamiltonian with a Subset of Normal Modes for Studying Mode-Specific Energy Transfer in Intermolecular Collisions<sup>†</sup>

Tianying Yan and William L. Hase\*

Department of Chemistry and Institute for Scientific Computing, Wayne State University,  
Detroit, Michigan 48202

Received: September 28, 2000; In Final Form: December 13, 2000

A Hamiltonian is described in which some degrees of freedom are represented by normal modes and the remainder retain their complete couplings and anharmonicities. The classical equations of motion for this Hamiltonian may be efficiently integrated in Cartesian coordinates. This Hamiltonian is used to study the mode specificity of energy transfer in Ne-atom collisions with alkanethiolate chains and a monolayer of *n*-hexyl thiolate chains self-assembled on Au{111}. The intermolecular and intramolecular degrees of freedom for these chain and self-assembled monolayer (SAM) systems are represented by normal modes. Collinear collisions with *n*-hexyl and *n*-octadecyl thiolate chains show that only one mode is excited at low collision energies. Mode specificity is also observed in Ne-atom collisions with the SAM. As expected from the adiabatic/impulsive model of  $T \rightarrow V$  energy transfer, higher frequency modes of the chains and monolayer are excited as the Ne-atom translational energy is increased. A comparison, between this normal mode model and an anharmonic surface model, suggests it is efficient energy transfer to highly anharmonic modes of the surface which give rise to the Boltzmann component in the translational energy distribution of the scattered Ne atoms.

## I. Introduction

Classical trajectories are widely used to determine atomic motions for a wide variety of studies including both equilibrium<sup>1</sup> and nonequilibrium molecular dynamics<sup>2,3</sup> and chemical reaction dynamics simulations.<sup>4,5</sup> A variety of different coordinate systems and Hamiltonians are used for these studies. For molecular systems with a small number of atoms, internal coordinates are practical for solving the classical equation of motion. However, as the number of atoms increases, they are less appropriate due to the complexity of the kinetic energy expression in an internal coordinate representation.<sup>6</sup> For large, many-atom systems it is most convenient to solve the classical equations of motion in Cartesian coordinates.

A particularly interesting question in molecular dynamics involves determining the mechanism(s) for collisional translation-to-vibration (i.e.,  $T \rightarrow V$ ) energy transfer.<sup>7</sup> This energy transfer process is important for numerous systems including collision-induced dissociation (CID) and surface-induced dissociation (SID) of biological molecules,<sup>8–10</sup> energy transfer in collisions of gases with surfaces,<sup>11,12</sup> and friction forces at the interfaces of sliding surfaces.<sup>2,3</sup> For the latter, the energy transfer is from the translational motion of the sliding coordinate to the vibrational modes of the surfaces. Different models have been advanced for describing  $T \rightarrow V$  in gas-phase and gas–surface collisions. Curvatures along an association/trapping reaction path have been used to describe couplings between reagent relative translation and vibrations orthogonal to the reaction path.<sup>13–15</sup> Resonance conditions are expected to facilitate this energy transfer.<sup>16–18</sup> The concept of adiabaticity may also be used to characterize the efficiency of  $T \rightarrow V$  energy transfer.<sup>19</sup> If the duration of an  $A + B$  collision,  $t_c$ , is short compared to the period of the vibrational motion to be excited,  $t_v$ , efficient energy

transfer is expected. The contrary is expected when the collision duration is long.<sup>19</sup>

To develop a complete and accurate model for such  $T \rightarrow V$  energy transfer processes requires determining the vibrational mode(s) initially excited by the intermolecular interaction. At low energies this may be done by transforming the Cartesian coordinates and momenta, used for solving the classical equations of motion, to normal mode coordinates and momenta. Though this transformation is only exact in the small displacement limit,<sup>20–22</sup> it still gives realistic results if the total energy is not too large.<sup>23</sup> Here one finds the difference between total energies calculated by the Cartesian and normal mode Hamiltonians is small. However, for the high energies in many collisional processes as CID<sup>8,9</sup> and SID,<sup>10</sup> this is not a viable approach for identifying the vibrational modes initially excited. Because of the linear transformation between the Cartesian and normal mode coordinates,<sup>20–22</sup> high total energies calculated by the Cartesian and normal mode Hamiltonians may differ by an order of magnitude or even more. This arises from the normal mode potential energy, since the kinetic energy is the same for the two coordinate systems.<sup>20,21</sup> If intramolecular vibrational energy redistribution (IVR)<sup>24</sup> does not occur for the collisionally excited molecule, energies in its individual normal modes may be determined by calculating the average kinetic energy  $\langle T_i \rangle$  for each of the modes<sup>25</sup> and then approximating the mode's energy  $E_i$  by  $2\langle T_i \rangle$ .<sup>26</sup> However, for many molecular systems IVR is rapid at both high and moderate energies,<sup>24,27</sup> and averaging  $\langle T_i \rangle$  over time is not a proper approach for determining a mode's initial energy or its time evolution.

An alternative approach for studying both the efficiency and mode specificity of intermolecular energy transfer is to use a Hamiltonian in which a subset of the degrees of freedom are represented by normal modes. Normal modes describe distinct vibrational motions and are a possible coordinate set to identify pathways for  $T \rightarrow V$  energy transfer. Though normal modes

<sup>†</sup> Part of the special issue "William H. Miller Festschrift".

\* Author to whom correspondence should be addressed.

are inadequate for describing intramolecular vibrational energy redistribution (IVR),<sup>24</sup> they may be useful for studying intermolecular energy transfer processes which occur on a time-scale much shorter than that for IVR. However, to use normal modes in classical trajectory simulations of  $T \rightarrow V$  pathways requires constructing a classical Hamiltonian which includes normal mode coordinates for intramolecular vibrations and nonnormal mode coordinates for the intermolecular degrees of freedom of the interacting species.

In the work presented here a Cartesian coordinate classical Hamiltonian, which represents a fraction of the degrees of freedom as normal modes, is described. Normal mode coordinates and the transformation between normal mode and Cartesian coordinates are briefly reviewed in Section II. In Section III strategies for integrating the Cartesian classical equations of motion are discussed for Hamiltonians in which all the degrees of freedom are normal modes and for Hamiltonians in which only a subset of the degrees of freedom are normal modes. In Section IV the latter type of Hamiltonian is used to study mode-specific energy transfer in high energy collinear collisions of Ne-atoms with alkanethiolates and in lower energy collisions of Ne-atoms with a *n*-hexyl thiolate self-assembled monolayer (SAM). These applications are motivated by experimental and computational studies of the efficiency of  $T \rightarrow V$  energy transfer in CID<sup>8,9</sup> and SID<sup>10</sup> and the recent computational finding that the Boltzmann component, in the translational energy distribution of Ne-atoms scattered off the *n*-hexyl thiolate SAM, does not arise from trapping desorption.<sup>12</sup> The work presented here addresses the applicability of a normal mode model for studying collisional energy transfer and the role of mode specificity in this transfer, and is summarized in Section V.

## II. Normal Mode Coordinates

The total energy of a polyatomic molecule, containing  $N$  atoms, may be written as

$$E = T + V = \sum_{i=1}^N \frac{m_i}{2} (\dot{x}_i^2 + \dot{y}_i^2 + \dot{z}_i^2) + V(x_1, y_1, \dots, z_N) \quad (1)$$

where the coordinates are defined with respect to a space-fixed axis system. To separate translational, rotational, and vibrational degrees of freedom, the coordinates of the atoms are defined with respect to a rotating axis system. The origin of this rotating system is the molecular center-of-mass. Using the Eckart (or Sayvetz) conditions to obtain  $3N$  independent coordinates for this rotating system,<sup>20,21</sup> the kinetic energy  $T$  in eq 1 becomes

$$2T = M\dot{R}^2 + \sum_i m_i (\boldsymbol{\omega} \times \mathbf{r}_i) \cdot (\boldsymbol{\omega} \times \mathbf{r}_i) + \sum_i m_i \dot{s}_i^2 + 2\boldsymbol{\omega} \cdot \sum_i m_i \mathbf{s}_i \times \dot{\mathbf{s}}_i \quad (2)$$

where  $M$  is the mass of the molecule,  $s_i$  is the instantaneous displacement of the  $i$ th atom from its equilibrium position, and  $\boldsymbol{\omega}$  is the angular velocity of the rotating system. The first three terms represent the pure translational, rotational, and vibrational kinetic energies, whereas the last term is the coupling between rotation and vibration; i.e., the Coriolis energy. To treat the vibrational and rotational motion of the molecule, the center-of-mass translational energy  $M\dot{R}^2$  may be set to zero and the origin of the rotating axis system placed at the origin of the space-fixed axis system without loss of generality.

If the angular velocity  $\boldsymbol{\omega}$  of the rotating coordinate system is small and the vibrational kinetic energy large, the Coriolis

energy term in eq 2 is much smaller than the vibrational kinetic energy  $T_v$  and it becomes a good approximation to identify this latter energy with the third term in eq 2; i.e.,

$$2T = \sum_i m_i \dot{s}_i^2 \quad (3)$$

where, for simplicity, the subscript  $v$  is dropped from  $T_v$ . To represent normal mode coordinates, it is convenient to use mass-weighted Cartesian coordinates  $q_i$  defined by  $q_i = \sqrt{m_i} s_i$ . The vibrational kinetic energy then takes the simpler form

$$2T = \sum_i \dot{q}_i^2 \quad (4)$$

Often it is sufficient to assume a quadratic intramolecular potential; i.e.,

$$2V = \sum_{ij} f_{ij} q_i q_j \quad (5)$$

In matrix notation, the above expressions for  $T$  and  $V$  become  $2T = \dot{\mathbf{q}}\dot{\mathbf{q}}$  and  $2V = \tilde{\mathbf{q}}\mathbf{f}\mathbf{q}$ , where the symbol  $\sim$  denotes the transpose and  $\mathbf{f}$  is a square  $3n \times 3n$  symmetric matrix of the mass-weighted Cartesian force constants  $f_{ij}$ . These expressions for  $T$  and  $V$  are transformed to diagonal form by a linear transformation between mass-weighted Cartesian coordinates  $q_i$  and normal mode coordinates  $Q_k$ ,<sup>28</sup> i.e.,

$$q_i = \sum_k l_{ik} Q_k \quad (6)$$

The transformation between the  $q_i$  and  $Q_k$  is written as  $\mathbf{q} = L\mathbf{Q}$ . The inverse transformation from Cartesian to normal mode coordinates is therefore  $\mathbf{Q} = L^{-1}\mathbf{q}$ , where  $L^{-1}$  is the inverse of  $L$ , i.e.,  $L L^{-1}$  equals  $\mathbf{E}$  the unity matrix. Since  $L$  is orthogonal,  $L^{-1} = \tilde{L}$ . With this transformation, both  $T$  and  $V$  have only diagonal components and are expressed as

$$2T = \dot{\mathbf{Q}}\dot{\mathbf{Q}} \quad (7)$$

and

$$2V = \tilde{\mathbf{Q}}\Lambda\mathbf{Q} \quad (8)$$

where  $\Lambda$  is a diagonal matrix whose elements are the normal-mode frequency parameters  $\lambda_k = 4\pi^2 c^2 \nu_k^2$ . These elements of  $\Lambda$  are the eigenvalues of the  $\mathbf{f}$  matrix. The columns of  $L$  are eigenvectors and give the transformation from Cartesian to normal mode coordinates. From the definition of momentum,<sup>29</sup>  $\dot{Q}_i$  is the momentum  $P_i$  for normal mode  $i$ .

## III. Cartesian Classical Equations of Motion

**A. All Degrees of Freedom Are Normal Modes.** The normal mode Hamiltonian  $H$  is separable and given by

$$H = \sum_i (P_i^2 + \lambda_i Q_i^2)/2 \quad (9)$$

The time-dependence of  $Q_i$  and  $\dot{Q}_i$  may be found by solving Newton's equation of motion and are

$$Q_i(t) = (2E_i/\lambda_i)^{1/2} \cos(\omega_i t + \delta_i) \quad (10)$$

and

$$P_i(t) = \dot{Q}_i(t) = -\omega_i(2E_i/\lambda_i)^{1/2} \sin(\omega_i t + \delta_i) \quad (11)$$

where  $\omega_i = 2\pi\nu_i$  and  $\delta_i$  is the phase factor for mode  $i$ . The time-dependence of the mass-weighted Cartesian coordinates  $q_i$  and velocities  $\dot{q}_i$  is then found from the  $Q_i(t)$  and  $\dot{Q}_i(t)$  by the linear transformation in eq 6. The resulting molecular angular momentum, given by

$$\mathbf{J} = \sum_i \mathbf{q}_i \times \dot{\mathbf{q}}_i \quad (12)$$

may not be zero and, if so, will vary with time. This is because the Coriolis energy term in eq 2 is not included in representing the molecule's vibrational/rotational energy and is the origin of the spurious angular momentum that arises in the transformation from normal mode to Cartesian coordinates.<sup>30,31</sup> However, since the angular velocity of the rotating coordinate system is small, both  $\mathbf{J}$  and the molecule's rotational energy are small.

The value for this spurious angular momentum depends on the normal mode(s) excited. There is no angular momentum if a single normal mode is excited. The excitation of two normal modes will contribute to  $\mathbf{J}$  in eq 12 if, according to group theory, the "product" of their symmetry types contains external rotation.<sup>32</sup> These effects are illustrated in Figure 1, for initial conditions in which zero-point energy is added to the normal modes of H<sub>2</sub>O. There is no angular momentum when zero-point energy is added to the individual normal modes or simultaneously to the bend and symmetric stretch. Parts a, b, and c of Figure 1 illustrate, respectively, the effect of adding zero-point energy to the asymmetric stretch and symmetric stretch, to the asymmetric stretch and bend, and to all three normal modes. For these excitation patterns, there is a time-dependent Cartesian coordinate angular momentum and rotational energy. The latter is calculated from

$$E_{\text{rot}} = \frac{\omega_m \cdot \mathbf{J}}{2} \quad (13)$$

where  $\omega_m$  is the angular velocity of H<sub>2</sub>O and not that of the rotating coordinate system. For all cases the rotational energy is small and at most constitutes less than one percent of the total energy.

The time-dependence of the Cartesian coordinates and velocities, associated with normal modes, may also be found by solving Hamilton's equations of motion<sup>33</sup>

$$\frac{\partial q_i}{\partial t} = \frac{\partial H}{\partial p_i}, \quad \frac{\partial p_i}{\partial t} = -\frac{\partial H}{\partial q_i} \quad (14)$$

where  $p_i = \dot{q}_i$  is the mass-weighted Cartesian momentum for coordinate  $i$ . From eqs 10 and 11 and the linear transformation between Cartesian and normal mode coordinates in eq 6, it is straightforward to write the derivatives  $\partial q_i/\partial t$  and  $\partial p_i/\partial t$ . Using the relation  $\sum p_i^2 = \sum P_i^2$  and the Hamiltonian in eq 9, Hamilton's equations of motion may also be expressed as

$$\frac{\partial q_i}{\partial t} = p_i \quad (15)$$

and

$$\frac{\partial p_i}{\partial t} = -\sum_j \lambda_j Q_j \frac{\partial Q_j}{\partial q_i} = -\sum_j \lambda_j I_{ji} Q_j \quad (16)$$

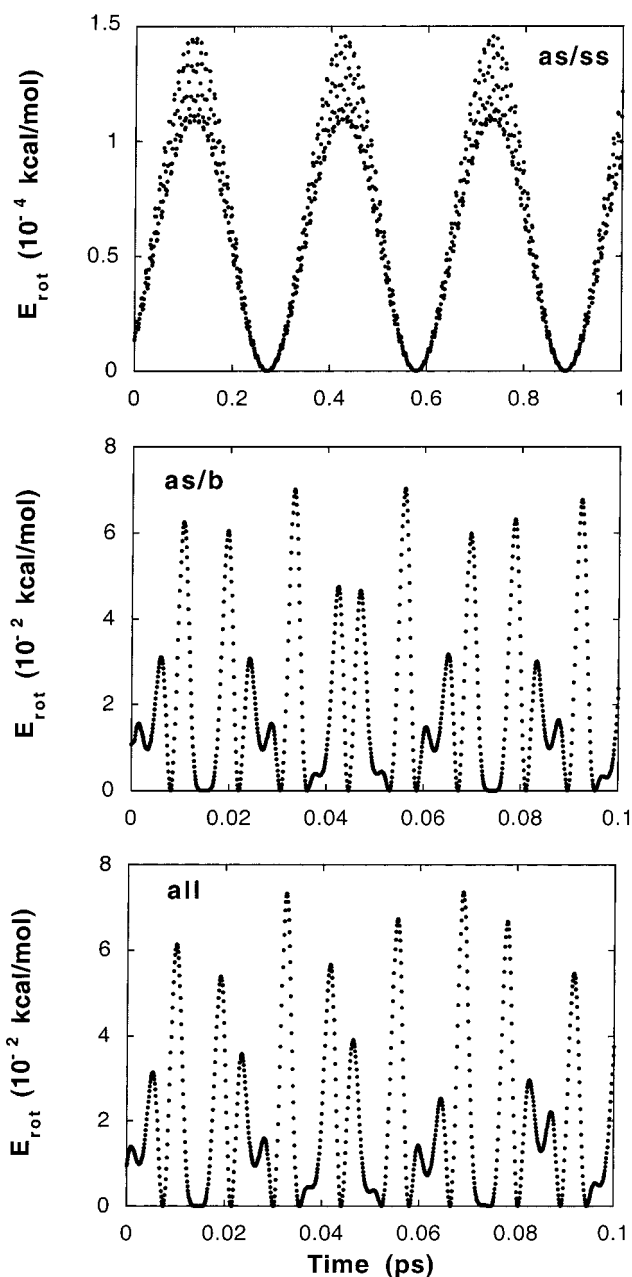


**Figure 1.** H<sub>2</sub>O rotational energy, when the normal mode coordinates and momenta of the normal mode Hamiltonian, eq 22, are transformed to Cartesian coordinates and momenta, eq 16. The plots are for different types of zero-point excitations: (a) - zpe in the asymmetric and symmetric stretch; (b) - zpe in the asymmetric stretch and bend; and (c) - all three modes are excited. The H<sub>2</sub>O harmonic frequencies are  $\omega_b = 1413 \text{ cm}^{-1}$ ,  $\omega_{ss} = 3614 \text{ cm}^{-1}$ , and  $\omega_{as} = 3668 \text{ cm}^{-1}$ .

Since eq 5 may be used to represent the potential energy,  $\partial p_i/\partial t$  may also be written as

$$\frac{\partial p_i}{\partial t} = \sum_j f_{ij} q_j \quad (17)$$

### B. A Subset of the Degree of Freedom Are Normal Modes.

The above normal mode Hamiltonian may be used to study the specificity of translation to vibration ( $T \rightarrow V$ ) energy transfer when two species collide. The normal mode Hamiltonian is used to represent the intramolecular degrees of freedom of the collision partners, while all couplings are included in the intermolecular potential. Since this normal mode model does

not allow for rotation, it may not be used to study collisions which transfer angular momentum. Rotational angular momentum and energy transfer may be included by using the complete Hamiltonian in eq 2 and this more detailed model will be treated in future work. However, the nonrotating model has a variety of applications, including collinear collisions and collisions with a surface, which are presented in the next section. This Hamiltonian, with a subset of the degrees of freedom as normal modes, may be illustrated by considering the collision of an atom with a surface. The surface, consisting of  $n$  atoms, is represented by the normal mode model and the  $n + 1$  atom is the colliding species. The Cartesian Hamiltonian for this system is

$$H = \sum_{i=1}^{3n} [P_i^2(\mathbf{p}) + \lambda_i Q_i^2(\mathbf{q})]/2 + \sum_{i=3n+1}^{3n+3} p_i^2/2 + V_{\text{inter}} \quad (18)$$

where  $\mathbf{p}$  and  $\mathbf{q}$  denote the  $3n$  Cartesian coordinates and momenta of the surface and  $V_{\text{inter}}$  is the intermolecular potential between the  $n$  atoms of the surface and the colliding  $n + 1$  atom. It is often sufficient to represent  $V_{\text{inter}}$  as a sum of two body potentials, only dependent on the distances between the surface atoms and the  $n + 1$  atom; i.e.,

$$V_{\text{inter}} = \sum_{i=1}^n V(r_{i,n+1}) \quad (19)$$

For efficient numerical solution of the classical equation of motion, the normal mode Hamiltonian for the surface may be explicitly expressed in terms of Cartesian coordinates and momenta and, thus, eq 18 becomes

$$H = \sum_{i=1}^{3n+3} p_i^2/2 + \sum_{ij}^{3n} f_{ij} q_i q_j/2 + V_{\text{inter}} \quad (20)$$

The classical equations of motion are eq 15 and

$$\begin{aligned} -\frac{\partial p_i}{\partial t} &= \sum_{j=1}^{3n} f_{ij} q_j + \frac{\partial V_{\text{inter}}}{\partial q_i}, \quad i \leq 3n \\ -\frac{\partial p_i}{\partial t} &= \frac{\partial V_{\text{inter}}}{\partial q_i}, \quad i = 3n + 1 \text{ to } 3n + 3 \end{aligned} \quad (21)$$

At any time, during the course of the trajectory, the individual normal mode energies of the surface may be determined by transforming the Cartesian  $q_i$  and  $p_i$  to normal mode  $Q_i$  and  $P_i$ .

#### IV. Applications

In the work presented here, the above model is used to study mode-specific energy transfer during direct, short-time collisions of Ne with alkanethiolate chains and the  $n$ -hexyl thiolate SAM. The simulations are performed by adding the normal mode Hamiltonian model to the chemical dynamics computer program VENUS.<sup>34</sup>

**A. Ne + Alkyl Thiolate Chains.** Collinear Ne-atom collisions with  $\text{CH}_3-(\text{CH}_2)_5-\text{S}-\text{M}_3$  and  $\text{CH}_3-(\text{CH}_2)_{17}-\text{S}-\text{M}_3$  chains are simulated at collision energies ranging up to 2500 kcal/mol, to represent the high collision energies often used in CID and SID experiments;<sup>8-10</sup> i.e., energies of 100 eV and more.<sup>35</sup> Collisional activation of excited electronic states is possible at these high energies. The simulations reported here pertain to vibrational excitation of the ground electronic state.

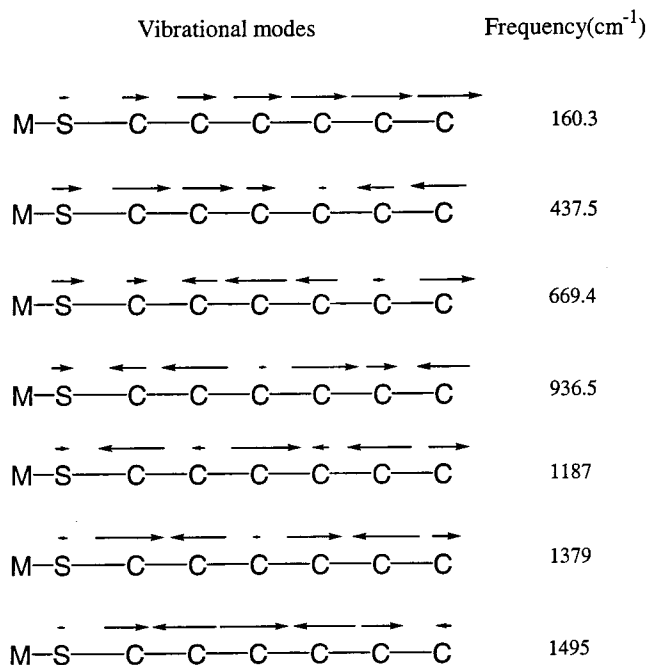


**Figure 2.** Eigenvectors and vibrational frequencies ( $\text{cm}^{-1}$ ) for the seven normal modes of vibration of the collinear  $(\text{C}')_6-\text{S}$  moiety.

The  $\text{CH}_3$  and  $\text{CH}_2$  moieties are represented by  $\text{C}'$  united-atoms (UAs) with masses of 15 and 14 amu, respectively, to form a collinear  $(\text{C}')_6-\text{S}$  chain attached to the center of a trigonal  $\text{M}_3$  plane. The M-atom was made sufficiently massive, i.e., 200 000 amu, so that the  $(\text{C}')_6-\text{S}-\text{M}_3$  moiety did not acquire an appreciable velocity as a result of a collision with the Ne-atom. The normal mode Hamiltonian for  $(\text{C}')_6-\text{S}-\text{M}_3$  was constructed using the same C-C, C-S, and S-M stretching force constants and equilibrium bond lengths used in the previous Ne-atom plus  $n$ -hexyl thiolate SAM simulations;<sup>36</sup> i.e., C-C,  $k_r = 4.86$  and  $r_o = 1.53$ ; C-S,  $k_r = 5.70$  and  $r_o = 1.82$ ; and S-Au,  $k_r = 2.80$  and  $r_o = 2.55$ , where  $k_r$  and  $r_o$  are in units of  $\text{mdyn}/\text{\AA}$  and  $\text{\AA}$ , respectively. The Cartesian force constants, eq 15, and eigenvectors and eigenvalues for the normal mode Hamiltonian are determined numerically by VENUS.<sup>34</sup> The seven normal modes of vibrations, for the collinear  $(\text{C}')_6-\text{S}$  moiety, are depicted in Figure 2 along with their vibrational frequencies. In ascending order, the frequencies are 62.0, 184.6, 303.3, 415.0, 519.6, 622.4, 727.3, 832.4, 934.7, 1032, 1123, 1206, 1281, 1347, 1404, 1450, 1487, 1513, 1528  $\text{cm}^{-1}$  for the  $(\text{C}')_{18}-\text{S}$  chain's nineteen normal modes of vibration.

The two-body intermolecular potential between Ne and the  $\text{C}'$  UA was determined previously<sup>36</sup> by ab initio calculations for  $\text{Ne}-\text{CH}_4$  and is excellently fit, for energies up to  $\sim 1000$  kcal/mol, by

$$V = a/r^{12} - b/r^6 + c \exp(-dr) + f/r^9 \quad (22)$$

with the fitted parameters given in ref 36. To represent very high energy Ne collisions, the ab initio calculations and fit were extended to greater than 10 000 kcal/mol to give the potential parameters  $a = 0.2172187$  kcal/mol  $\text{\AA}^{12}$ ,  $b = 88.42075$  kcal/mol  $\text{\AA}^6$ ,  $c = 88.42075$  kcal/mol,  $d = 88.42075$   $\text{\AA}^{-1}$ , and  $f = 88.42075$  kcal/mol  $\text{\AA}^9$ . These parameters are used for the trajectory results presented here.

Calculations are performed for collinear Ne collisions with the alkanethiolate chains using two different sets of initial conditions. For one set no initial energy is added to the chain,

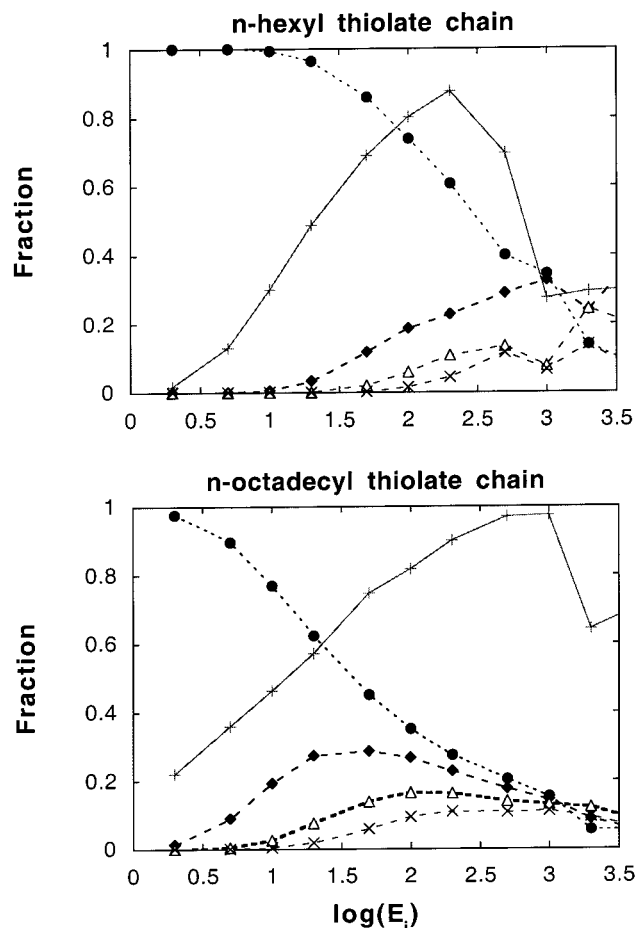


**Figure 3.** Fraction of the initial Ne translational energy  $E_i$  transferred to the alkanethiolate chain is given by the (+) points and (-) line. Also plotted are the fractions of this transferred energy deposited in the 4 modes receiving the most energy at low  $E_i$ . For  $(C'_6-S-M_3)$  these modes, identified by their frequencies ( $\text{cm}^{-1}$ ), are 160.3 (-●-); 437.5 (-◆-); 669.4 (-△-); and 936.5 (-×-). For  $(C'_{18}-S-M_3)$  these modes are: 62.0 (-●-); 184.6 (-◆-); 303.3 (-△-); and 415.0 (-×-). The initial conditions with and without zero-point energy in the alkanethiolate chain given the same result.

so that it is in its classical potential energy minimum. Thus, for each  $E_i$  there is only one unique trajectory. For the other set of initial conditions, zero-point energy is added to the chain, with random phases of the normal mode coordinates and momenta.<sup>37</sup> A very important finding from these two sets of calculations is that the initial condition without energy added to the alkanethiolate chain gives the same energy transfer to each mode as the average found for the initial conditions with zero-point energy added to the chain. In Figure 3 the average fraction of  $E_i$  transferred to  $(C'_6-S-M_3)$  and  $(C'_{18}-S-M_3)$  is plotted versus  $\log E_i$  for  $E_i$  up to 2500 kcal/mol. For both chains this fraction first increases, approaching unity, and then decreases before increasing again. The distribution  $P(E_f)$  of the final Ne-atom translational energy  $E_f$  is plotted in Figure 4 for the Ne +  $(C'_6-S-M_3)$  collisions with zero-point energy and  $E_i$  in the range of 2 to 500 kcal/mol. For  $E_i$  greater than 500 and as large as 2500 kcal/mol, the shapes of  $P(E_f)$  are similar to the one for  $E_i = 500$  kcal/mol.

At low  $E_i$ , where the energy transfer is predominately to one mode,  $P(E_f)$  is concave. However, with increase in  $E_i$  and more modes becoming excited,  $P(E_f)$  undergoes a transition to a convex shape. The shape of  $P(E_f)$  at low energy reflects the probability distribution of the coordinate of the normal mode which is excited. The coordinate's most probable values are

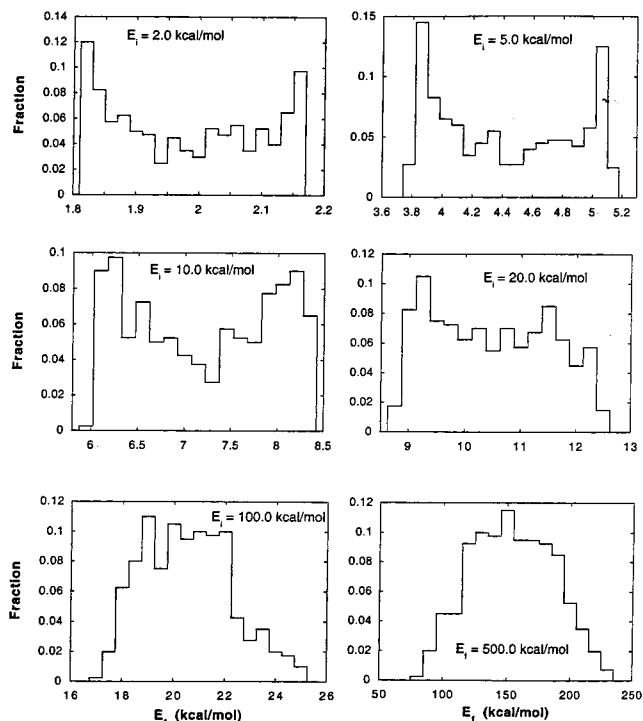


**Figure 4.** Distribution of the final Ne atom translational energy  $E_f$  for Ne +  $(C'_6-S-M_3)$  collisions with zero-point energy in the alkanethiolate chain.

those for its inner and outer turning points, at which the amount of energy transferred tends to be smallest and largest, respectively.

At low values of  $E_i$  the energy transfer to the alkanethiolate chain is very mode specific. This is shown in Figure 3, where the fractions of the transferred energy deposited in the four modes receiving most of the energy at low  $E_i$  are plotted versus  $\log E_i$ . For the smaller  $(C'_6-S-M_3)$  chain and  $E_i$  less than 30 kcal/mol, more than 90% of the energy is transferred to the mode with the lowest frequency. For the larger  $(C'_{18}-S-M_3)$  chain this type of mode-specific energy transfer is restricted to energies less than 6 kcal/mol. As  $E_i$  is increased, more modes become excited and there is less mode specificity. At the highest energy,  $E_i = 2500$  kcal/mol, the average fractions of the transferred energy deposited into 7 modes of  $(C'_6-S-M_3)$  and 19 modes of  $(C'_{18}-S-M_3)$  are 0.109, 0.284, 0.253, 0.112, 0.056, 0.172, and 0.015, and 0.053, 0.069, 0.095, 0.068, 0.037, 0.058, 0.094, 0.120, 0.129, 0.107, 0.054, 0.025, 0.040, 0.018, 0.018, 0.007, 0.003, 0.001, and 0.000, respectively, for the frequencies in ascending order. However, even at this high  $E_i$ , there is still some degree of mode selectivity.

The mode-specific energy transfer observed in these simulations is very important and raises significant questions about the dynamics of collisional energy transfer. Figure 3 shows that at low collision energy the lowest frequency mode, whose principal motion involves symmetric elongation/compression of the alkanethiolate chain, receives most of the energy. As the collision energy is increased, the remaining modes, in ascending order based on their vibrational frequencies, become excited. At the highest collision energy considered here, 2500 kcal/mol, a number of the modes of both the  $n$ -hexyl and  $n$ -octadecyl chains are excited. However, as shown above, even for this high energy collision, energy transfer to the modes is far from democratic. The specific modes, receiving most of the energy, depend on the modes' atomic motions and frequencies. As the collision energy is increased, there is a tendency for excitation

of higher frequency modes. It is noteworthy that the mode-specific collisional energy transfer found in these simulations may assist in explaining a recent experimental finding of nonstatistical dissociation of collisionally activated  $\text{CH}_3\text{SH}^+$  and  $\text{CH}_3\text{CH}_2\text{SH}^+$ .<sup>38</sup>

**B. Ne + *n*-Hexyl Thiolate SAM.** The mode specificity of energy transfer in collisions of Ne atoms with the *n*-hexyl thiolate SAM/Au{111} surface was studied by using the normal mode Hamiltonian to represent the surface's vibrational degrees of freedom. The results of this simulation are also compared with those obtained when the complete potential is used for the surface, instead of truncating this potential at the quadratic terms. This complete surface potential was used in our previous simulations of Ne and *n*-hexyl thiolate SAM/Au{111} collisions.<sup>12,36</sup>

There have been extensive studies of energy transfer in collisions with organic liquids<sup>11,39–44</sup> and self-assembled monolayers<sup>12,36,45</sup> and it is important to have a deeper understanding of energy transfer in these systems. In collisions of Ne-atoms with liquid squalane, it is found that approximately 70% of the collision energy is transferred to the liquid at high collision energies.<sup>44</sup> A similar energy transfer efficiency is found in a computer simulation of Ne-atom collisions with *n*-hexyl thiolate self-assembled on Au{111}.<sup>12,36</sup> The energy transfer distribution for collisions of Ne with both this SAM and liquid squalane, may be similarly deconvoluted into a Boltzmann distribution based on the surface temperature and a remaining high energy component.<sup>36,44</sup> The origin of the Boltzmann component is particularly intriguing, since the simulations show a trapping-desorption intermediate is unimportant for the Ne + SAM collisions.<sup>12</sup> The statistical-like angular distribution of scattered Ne atoms arises from the surface roughness.<sup>12</sup> In the work presented here, collisions of Ne-atoms with the *n*-hexyl thiolate SAM normal mode model are simulated, to see if the mode-specific energy transfer dynamics provides insight into the origin of the Boltzmann component in the energy transfer distribution.

The same surface model, with 35 alkanethiolate chains and C' UAs for the  $\text{CH}_3$  and  $\text{CH}_2$  groups of the chain, were used here as in previous simulations<sup>12,36</sup> of Ne + SAM/Au{111} collisions. The analytic potential energy function is also the same as used previously, and consists of terms for the SAM intermolecular and intramolecular potentials, the S–Au interactions, the interactions between Ne and the methyl and methylene UAs of the SAM. The S-atoms of the chains are adsorbed on hollow sites of a rigid Au{111} surface. The resulting SAM monolayer forms a commensurate ( $\sqrt{3} \times \sqrt{3}$ )  $R30^\circ$  structure, which has a  $28^\circ$  tilt-angle between the Au{111} surface normal and the backbone of the  $\text{CH}_3(\text{CH}_2)_5\text{S}$  moiety, in excellent agreement with experiment.<sup>46,47</sup> (This surface model is depicted in Figure 1 of ref 36).

Initial conditions are chosen for the trajectories so that the incident Ne atoms are randomly aimed in the central unit area of the SAM surface. The initial velocity vectors of the Ne atoms are parallel with the  $28^\circ$  tilt-angle of the alkanethiolate chains. No initial energy is added to the SAM, so that it is in its classical potential energy minimum. Previous calculations<sup>12b</sup> have shown that the results for this initial condition are similar to those with a quasiclassical 300 K Boltzmann distribution. Calculations are performed with initial Ne translational energies  $E_i$  of 5 and 20 kcal/mol.

$P(E_f)$  distributions, of the final translational energy  $E_f$  of the scattered Ne atoms, are compared in Figure 5 for the simulations based on the anharmonic potential energy model for the SAM<sup>36</sup>

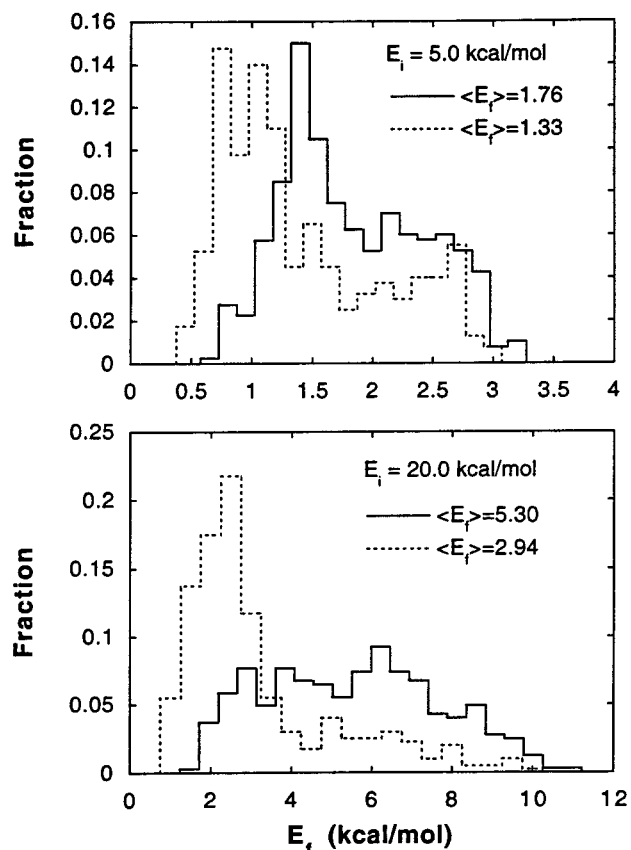


**Figure 5.** Distribution of the final Ne-atom translational energy  $E_f$  for  $E_i$  of 5 and 20 kcal/mol, and normal mode (—) and anharmonic (---) models for the SAM surface.

and the normal mode model described above. For  $E_i$  equal to 5 kcal/mol, the two models give similar  $P(E_f)$  distributions. They are peaked at low  $E_f$ , with an average final Ne translational energy that is 27 and 35% of  $E_i$  for the anharmonic and normal mode models of the SAM, respectively. For the higher  $E_i$  of 20 kcal/mol, the  $P(E_f)$  distributions of the two models are qualitatively different. The normal mode model gives a broad, flat distribution of final energies while the anharmonic model distribution is sharply peaked at low  $E_f$  with a long, small tail at higher  $E_f$ . This leads to a significantly low  $\langle E_f \rangle$  value (by a factor of 1.8) for the anharmonic model. The average final Ne translational energy is 15 and 26% of  $E_i$  for the anharmonic and normal mode surface models, respectively. Both surface models give an increase in the percent energy transfer to the surface as  $E_i$  is increased, the expected result.<sup>36</sup>

The major difference between the results, for the two surface models, is that low  $E_f$  values are less probable for the normal mode surface model. Including anharmonicity in the surface model is expected to have the greatest effect on the motions of the low frequency interchain vibrational frequencies and the smallest effect on the higher frequency intramolecular vibrations of the chains. Thus, the implication from this comparison of energy transfer for the two surface models is that it is efficient energy transfer to highly anharmonic interchain modes which gives rise to the Boltzmann component in  $P(E_f)$ . This Boltzmann component is observed when the azimuthal angle of the beam of Ne-atoms is chosen randomly to represent the situation where the SAM domain on which the atoms collide is not specified.<sup>12,36</sup>

The calculations with the normal mode model give the amount of energy initially deposited in each vibrational mode of the SAM by the Ne-atom collision. Figure 6 gives a scatter plot of the average energy  $\langle E_{\text{mode}} \rangle$  deposited in a SAM vibrational mode

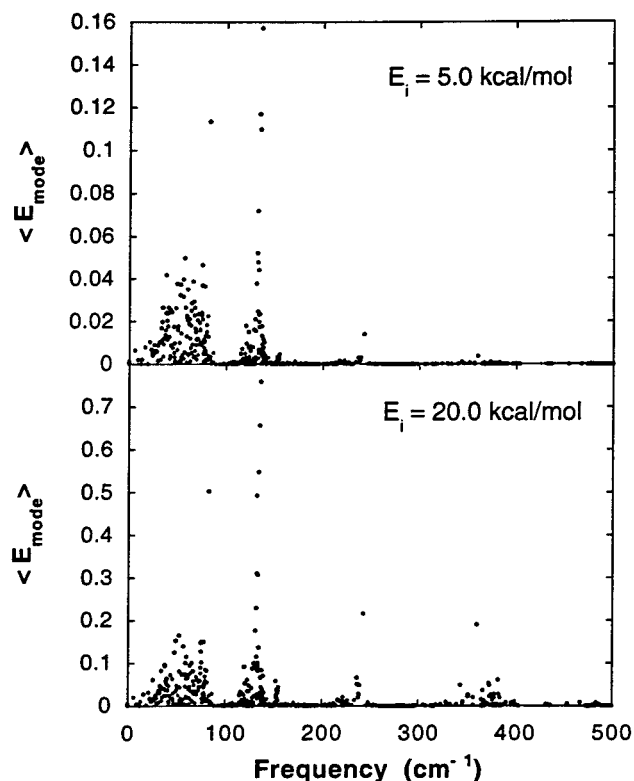


**Figure 6.** Scatter plot of the average energy deposited in a SAM vibrational mode versus the mode's vibrational frequency.  $E_{\text{mode}}$  is in kcal/mol.

versus the mode's vibrational frequency, for initial Ne-atom translational energies  $E_i$  of 5 and 20 kcal/mol. As  $E_i$  is increased, modes with higher vibrational frequencies are excited, in accord with the impulsive/adiabatic model of  $T \rightarrow V$  energy transfer.<sup>48</sup> However, somewhat surprisingly, the same five modes are most highly excited at both  $E_i$  of 5 and 20 kcal/mol. In ascending frequency, these modes are 82.6, 132.6, 134.2, 135.1, and 136.3  $\text{cm}^{-1}$ . If the next five most highly excited modes are considered, one sees the trend to excite higher frequency modes as  $E_i$  is increased. These five modes are 37.9, 56.8, 74.9, 132.0, and 132.5  $\text{cm}^{-1}$  at  $E_i = 5.0$  kcal/mol, and 132.0, 132.5, 133.5, 242.9, and 360.8  $\text{cm}^{-1}$  at  $E_i = 20$  kcal/mol. For  $E_i = 5.0$  kcal/mol there is only one mode with a frequency greater than 150  $\text{cm}^{-1}$  appreciably excited and for  $E_i = 20$  kcal/mol there is no appreciable excitation of modes with frequencies above 400  $\text{cm}^{-1}$ .

The distributions of energy deposited in the five most highly excited modes are plotted in Figure 7 for  $E_i = 5.0$  kcal/mol. Also given in this Figure are the average energies in each of the modes. Listed by ascending frequency, the average percent energy transfers to these five modes are 2.3, 1.4, 2.3, 2.1, and 3.1 at  $E_i = 5.0$  kcal/mol and 2.5, 2.5, 2.7, 3.3, and 3.8 at  $E_i = 20$  kcal/mol. Each of these vibrational modes involves movement of the atoms in the central unit area of the SAM struck by the Ne-atom. The predominant nature of the atomic motions associated with these five modes are asymmetric bending of the rows of alkanethiolate chains (82.6), CCC torsions and wagging of central chains (132.6), CCC torsions (134.2), CCC torsions (135.1), and CCC bending of central chains (136.3). Thus, the most highly excited modes consist of a varied range of motions.

A discussion was given in the Introduction of the merits of determining the mode specificity of the energy transfer by performing the dynamics with the fully anharmonic Hamiltonian

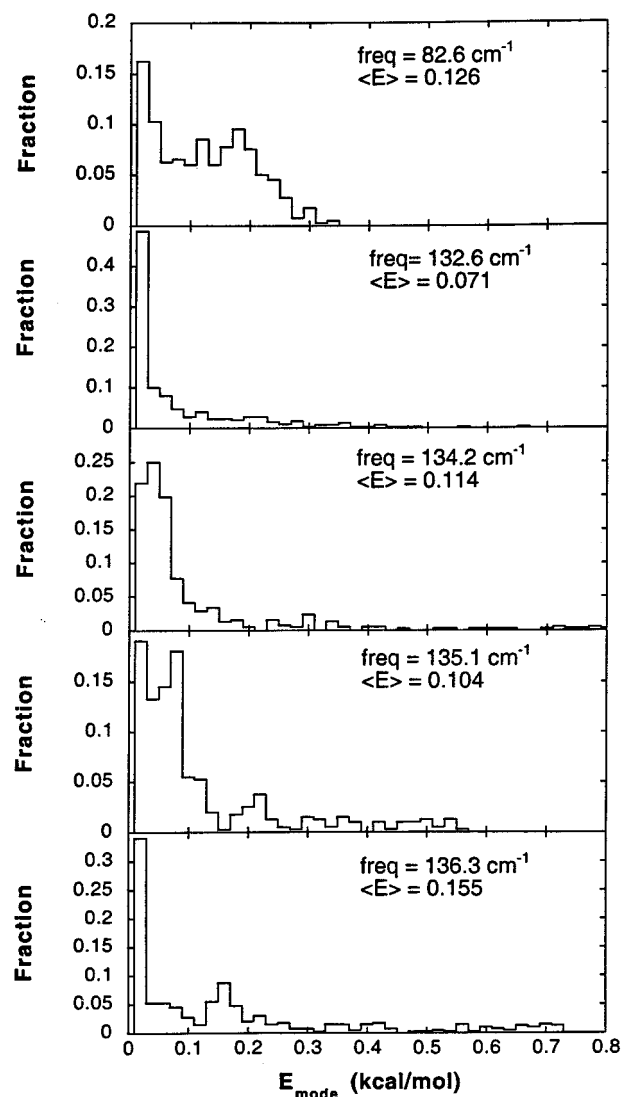


**Figure 7.** Distributions of energy deposited in the SAM's most highly excited modes.  $\langle E_i \rangle$  is the average energy in the mode.  $E_i = 5.0$  kcal/mol.

and then, after the collision, projecting the Cartesian coordinates and momenta onto the normal modes. This approach cannot be used to identify the modes of the SAM initially excited. Because of the linear transformation between Cartesian and normal mode coordinates, the SAM energies before and after this transformation are much different. The total normal mode energy fluctuates with time and is up to 5–10 times larger than that for the fully anharmonic Hamiltonian. As discussed in the Introduction, this is a well-known problem. In addition, because of IVR, the energies in individual normal modes may not be determined by tracking their kinetic energies. This is shown in Figure 8, where the kinetic energy is plotted versus time for collisions with  $E_i$  of 20 kcal/mol. The plots on the left, for the normal mode Hamiltonian, show that the collision and excitation of the mode require approximately 0.5 ps. The projected normal mode kinetic energies on the right, for the anharmonic Hamiltonian, are not periodic and exhibit energy transfer between normal modes. Though calculating the dynamics with the fully anharmonic Hamiltonian and projecting onto the normal mode may not be used to determine the mode energies, this approach does show that only the low-frequency modes are excited, as for the calculations with the normal mode Hamiltonian, and that IVR occurs between these modes.

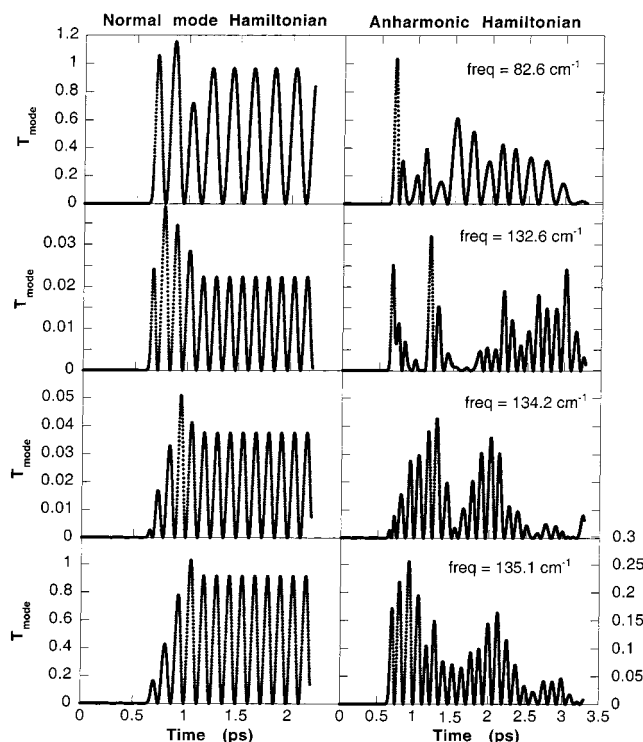


**Figure 8.** Plots of the kinetic energy versus time for the four SAM modes most highly excited in the calculations with the normal mode Hamiltonian. For the calculations with the fully anharmonic Hamiltonian, the energies for the modes were determined by projecting onto the normal mode coordinates and momenta.  $E_i = 20.0$  kcal/mol and  $T_{\text{mode}}$  is in kcal/mol.

## V. Summary

The following are the important findings from this work, concerning the use of normal mode Hamiltonians for studying collisional energy transfer and the energy transfer dynamics associated with Ne-atom collisions with *n*-hexyl thiolate chains.

1. A Hamiltonian may be constructed to study mode-specific energy transfer in collisional processes by treating the internal degrees of freedom of the colliding moieties as normal modes and using the complete anharmonic potential to represent the intermolecular interaction between these moieties. The classical equations of motion for this Hamiltonian may be efficiently integrated in Cartesian coordinates.

2. For low energy collinear collisions of Ne-atoms with the *n*-hexyl and *n*-octadecyl thiolate chains, energy is preferentially transferred to the lowest frequency mode. As the collision energy  $E_i$  is increased, in succession and according to their frequencies, higher frequency modes begin to become excited. At high  $E_i$  the energy transfer become less mode specific, but some mode specificity remains for  $E_i$  as large as 110 eV.

3. Energy transfer is also mode specific for collisions of the Ne-atom with a *n*-hexyl thiolate monolayer self-assembled on Au{111}. The modes excited involve motions of atoms in the area of the SAM struck by the Ne-atom. Excitation of higher frequency modes becomes more important as  $E_i$  is increased. For both collisions with the alkyl chain and the SAM, the specific modes excited depends on the modes' atomic motions and frequencies.

4. For  $E_i$  less or equal to 20 kcal/mol, the C–C stretching modes of the monolayer are not excited. This indicates a united-model is appropriate for representing the C–H stretching and bending modes of the CH<sub>3</sub> and CH<sub>2</sub> moieties of the alkyl chain for  $E_i$  in this energy range.

5. Energy transfer to the monolayer is compared for calculations with the normal mode and complete anharmonic models for the intramolecular and intermolecular motions of the monolayer. At low  $E_i$  the two models give similar  $P(E_f)$  distributions of the final Ne translational energy, which have a peak in  $E_f$  at low  $E_i$ . For higher  $E_i$ ,  $P(E_f)$  retains the same form for the anharmonic model, but becomes broad without a peak for the normal mode model. For both low and high  $E_i$ , the normal mode model gives a smaller probability for Ne-atoms scattering from the monolayer with a small final translational energy  $E_f$ . This result suggests it is efficient energy transfer to highly anharmonic modes of the monolayer which gives rise to the Boltzmann component in the translational energy distribution of the scattered Ne-atoms, as observed in previous trajectory simulations.<sup>12,36</sup>

Finally, in future work it would be of interest to consider several extensions of the work reported here. Instead of expressing the normal mode Hamiltonian as a linear transformation between normal mode and Cartesian coordinates, it could be expressed as a linear transformation between normal mode and curvilinear internal coordinates, with the internal coordinates written as analytic functions of Cartesian coordinates. It would also be worthwhile to investigate how including separable anharmonic terms in the normal mode potential energies affects the efficiency of energy transfer.

**Acknowledgment.** This research was supported by the National Science Foundation and the Office of Naval Research.

## References and Notes

- (1) Stanton, R. V.; Miller, J. L.; Kollman, P. A. In *Modern Methods for Multidimensional Dynamics Computations in Chemistry*; Thompson, D. L., Ed.; World Scientific: London, 1998; p 355.
- (2) Landman, U.; Luedtke, W. D.; Nitzan, A. *Surf. Sci.* **1989**, *210*, L177.
- (3) Mann, D. J.; Hase, W. L. *Tribology Lett.* **1999**, *7*, 153.
- (4) Bunker, D. L. *Methodol. Comput. Phys.* **1971**, *10*, 287.
- (5) Raff, L. M.; Thompson, D. L. In *Theory of Chemical Reaction Dynamics*; Baer, M., Ed.; CRC Press: Boca Raton, FL, 1985; Vol. 3, p 1.
- (6) Wilson, E. B., Jr.; Decius, J. C.; Cross, P. C. *Molecular Vibrations*; McGraw-Hill: New York, 1955; p 303.
- (7) Yardley, J. T. *Introduction to Molecular Energy Transfer*; Academic Press: New York, 1980; p 95.
- (8) Klassen, J. S.; Kebarle, P. *J. Am. Chem. Soc.* **1997**, *119*, 6552.
- (9) Meroueh, O.; Hase, W. L. *J. Phys. Chem. A* **1999**, *103*, 3981.
- (10) Cooks, R. G.; Ast, T.; Pradeep, T.; Wysocki, V. *Acc. Chem. Res.* **1994**, *27*, 316. (b) Vekey, K.; Somogyi, A.; Wysocki, V. *H. J. Mass Spectrom.* **1995**, *30*, 212. (c) Lim, H.; Schultz, D. G.; Yu, C.; Hanley, L. *Anal. Chem.* **1999**, *13*, 2307.
- (11) Saecker, M. E.; Govoni, S. T.; Kowalski, D. V.; King, M. E.; Nathanson, G. M. *Science* **1991**, *252*, 1421.
- (12) Yan, T.-Y.; Hase, W. L. *Phys. Chem. Chem. Phys.* **2000**, *2*, 901.
- (13) Yan, T.-Y.; Hase, W. L.; Barker, J. R. *Chem. Phys. Lett.* **2000**, *329*, 84.
- (14) Miller, W. H.; Smith, F. T. *Phys. Rev. A* **1978**, *17*, 939. (b) Miller, W. H. *J. Phys. Chem.* **1983**, *87*, 3811.
- (15) Dunning, T. H., Jr.; Kraka, E.; Eades, R. A. *Faraday Discuss. Chem. Soc.* **1987**, *84*, 427.
- (16) Wang, H.; Hase, W. L. *Chem. Phys.* **1996**, *212*, 247.
- (17) Song, K.; de Sainte Claire, P.; Hase, W. L.; Hass, K. C. *Phys. Rev. B* **1995**, *52*, 2949.
- (18) Heller, E. J.; Stechel, E. B.; Davis, M. J. *J. Chem. Phys.* **1980**, *73*, 4720.
- (19) Sibert, E. L.; Reinhardt, W. P.; Hynes, J. T. *J. Chem. Phys.* **1984**, *81*, 1115.
- (20) Levine, R. D.; Bernstein, R. B. *Chemical Reaction Dynamics and Chemical Reactivity*; Oxford: New York, 1987; p 312.
- (21) Wilson, E. B., Jr.; Decius, J. C.; Cross, P. C. *Molecular Vibrations*; McGraw-Hill: New York, 1955; p 273.
- (22) Califano, S. *Vibrational States*; Wiley: New York, 1976; p 16.
- (23) Flygare, W. F. *Molecular Structure and Dynamics*; Prentice Hall: Englewood Cliffs, NJ, 1978; p 39.

- (23) Hase, W. L.; Ludlow, D. M.; Wolf, R. J.; Schlick, T. *J. Phys. Chem.* **1981**, *85*, 958.
- (24) *Advances in Classical Trajectory Methods, Vol. 1, Intramolecular and Nonlinear Dynamics*; Hase, W. L., Ed.; JAI: London, 1992.
- (25) Raff, L. M. *J. Chem. Phys.* **1988**, *89*, 5680.
- (26) For an anharmonic system the average kinetic and potential energies are not necessarily equal as is the case for a harmonic system; Schiff, L. I. *Quantum Mechanics*, 3rd ed.; McGraw-Hill: New York, 1968; p 180. Hase, W. L.; Wolf, R. J.; Sloane, C. S. *J. Chem. Phys.* **1979**, *71*, 2911.
- (27) Lu, D. -h; Hase, W. L. *J. Chem. Phys.* **1988**, *89*, 6723.
- (28) Califano, S. *Vibrational States*; Wiley: New York, 1976; p 23.
- (29) Goldstein, H. *Classical Mechanics*; Addison-Wesley: London, 1950; p 48.
- (30) Chapman, S.; Bunker, D. L. *J. Chem. Phys.* **1975**, *62*, 2890.
- (31) Sloane, C. S.; Hase, W. L. *J. Chem. Phys.* **1977**, *66*, 1523.
- (32) Herzberg, G. *Molecular Spectra and Molecular Structure II*; Van Nostrand Reinhold: New York, 1945; p 376.
- (33) Hase, W. L.; Ludlow, D. M.; Wolf, R. J.; Schlick, T. *J. Phys. Chem.* **1981**, *85*, 215.
- (34) Hase, W. L.; Duchovic, R. J.; Hu, X.; Komornicki, A.; Lim, K. F.; Lu, D. -h; Peslherbe, G. H.; Swamy, K. N.; Vande Linde, S. R.; Varandas, A.; Wang, H.; Wolf, R. J. *QCPE* **1996**, *16*, 671.
- (35) Burroughs, J. A.; Wainhaus, S. B.; Hanley, L. J. *J. Phys. Chem.* **1994**, *98*, 10913.
- (36) Bosio, S. B. M.; Hase, W. L. *J. Chem. Phys.* **1997**, *107*, 9677.
- (37) Peslherbe, G. H.; Wang, H.; Hase, W. L. In *Advances in Chemical Physics*, Vol. 105; Ferguson, D. M., Siepmann, J. I., Truhlan, D. G., Eds.; Wiley: New York, 1999; p 171.
- (38) Chen, Y.-J.; Fenn, P. T.; Stimson, S.; Ng, C. Y. *J. Chem. Phys.* **1997**, *106*, 8274. Chen, Y.-J.; Stimson, S.; Fenn, P. T.; Ng, C. Y.; Li, W.-K.; Ma, N. L. *J. Chem. Phys.* **1998**, *108*, 8020.
- (39) King, M. E.; Nathanson, G. M.; Hanning-Lee, M. A.; Minton, T. K. *Phys. Rev. Lett.* **1993**, *70*, 1026.
- (40) Benjamin, I.; Wilson, M.; Pohorille, A. *J. Chem. Phys.* **1994**, *100*, 6500.
- (41) Lipkin, N.; Gerber, R. B.; Moiseyev, N.; Nathanson, G. M. *J. Chem. Phys.* **1994**, *100*, 8408.
- (42) Nathanson, G. M.; Davidovits, P.; Warsnop, D. R.; Kolb, C. E. *J. Phys. Chem.* **1996**, *100*, 13007.
- (43) King, M. E.; Fiehrer, K. M.; Nathanson, G. M.; Minton, T. K. *J. Phys. Chem. B* **1997**, *101*, 6556.
- (44) Saecker, M. E.; Nathanson, G. M. *J. Chem. Phys.* **1993**, *99*, 7056.
- (45) Cohen, S. R.; Naaman, R.; Sagiv, *Phys. Rev. Lett.* **1987**, *58*, 1208.
- (46) Porter, M. D.; Bright, T. B.; Allara, D. L.; Chidsey, C. E. D. *J. Am. Chem. Soc.* **1987**, *109*, 3559.
- (47) Camilone, N., III; Chidsey, C. E. D.; Eisenberger, P.; Fenter, P.; Li, J.; Lian, K. S.; Liu, G.-Y.; Scoles, G. *J. Chem. Phys.* **1993**, *99*, 744.
- (48) Levine, R. D.; Bernstein, R. B. *Chemical Reaction Dynamics and Chemical Reactivity*; Oxford: New York, 1987; p 31.